

## Parametric Study of MINOS Sensitivity to $\nu_\mu \rightarrow \nu_e$ Oscillations

Stanley Wojcicki

Stanford University

### ABSTRACT

We have performed a study of MINOS sensitivity to  $\nu_\mu \rightarrow \nu_e$  oscillations to various changes in the geometrical parameters of the NuMI beam, eg decay pipe length, target dimensions, target position, horn current, and separation between the two horns. The only parameters that suggest that an improvement may be possible, at the level of about 10% in the Figure of Merit, are the target dimensions and target position. The basic assumptions adopted for the parametric representation of the measurement errors and of reaction identification lead to a significantly lower background level from the high energy NC events than was calculated in NuMI-714.

## **Introduction.**

This note describes comparison studies between different beam configurations with respect to sensitivity to  $\bar{\nu}_\mu \rightarrow \nu_e$  oscillations in the MINOS detector and a generalized NuMI low energy beam. We start with the full fledged GNuMI simulation to generate neutrino fluxes at the Far Detector. The detection efficiencies for the signal, as well as background rejections, are however parametrized, the parametrizations being based on previous neutrino experimental results as well as previous simulation studies using full GEANT.

The specific beam parameters we address are: horn currents, position of the target with respect to the first horn, target dimensions, separation between the two horns, and length of the decay pipe. The approximations resulting from using a parametrized Monte Carlo probably do not influence significantly our comparisons even though they might not provide optimum level of accuracy for the absolute sensitivities.

## **Procedure and Parametrizations.**

The input to our calculations are the fluxes as calculated by the standard GNuMI GEANT3 based simulation program. The  $\bar{\nu}_\mu$  and  $\bar{\nu}_\mu$ -bar fluxes are propagated to the MINOS far detector located 735 km away using  $\Sigma m^2$  of  $3 \times 10^{-3} \text{ eV}^2$ , 100%  $\bar{\nu}_\mu$  disappearance probability at oscillation maximum, and 2% (approximately 2.5 times below the CHOOZ limit[1] ) probability of conversion to  $\nu_e$ 's or  $\bar{\nu}_e$ -bar's respectively, at the oscillation maximum.

It is assumed that the neutrino  $y$  distribution is flat and the antineutrino  $y$  distribution follows the  $(1-y)^2$  dependence independent of energy, for both charged and neutral current interactions; neutrino-antineutrino cross sections are taken to be equal at  $y=0$ . The neutrino cross section is taken to be linear with energy, the coefficient used being  $7 \times 10^{-38} \text{ cm}^2/\text{GeV}$  [2]. The ratio of total NC to CC cross sections is taken as 0.31 for both neutrinos and antineutrinos.

The detection efficiency for  $\bar{\nu}_e$  identification is taken as 30% independent of energy, the absolute value taken to be consistent with the previous work using full GEANT simulation for this energy range and described in NuMI-L-290 [3] as well as the efficiency in the energy of interest given in Fig.16 of NuMI-L-714 [4]. The same detection efficiency is assumed for  $\bar{\nu}_e$ -bar's, very likely a significant underestimate which is however probably not important for this work in light of a relatively small fraction of antineutrinos in the beam.

It is assumed that CC events can be identified as such (and thus do not contribute to the background) if the muon has an energy above 1.0 GeV. The CC events with a muon below this energy cutoff are assumed to have a probability of 2% of satisfying  $\bar{\nu}_e$  identification criteria. The probability that an NC event will satisfy these criteria is also taken to be 2%. Again, these numbers represent a rough average over the energies of interest for the results derived in the work described in NuMI-L-290 as well as in NuMI-L-714.

The detected energy for both signal and potential background events is smeared according to the algorithm  $\Delta E/E = 0.45/\sqrt{E}$ , where  $E$  is the true hadronic energy (including the muon if its energy lies below 1.0 GeV/c). This may be somewhat pessimistic for the signal since the electron energy determination is significantly more

accurate. Whether better energy definition can be achieved needs to be studied with more detailed simulations using more sophisticated algorithms.

The contribution to the background from  $\pi$  production and subsequent  $\pi$  decay, either to electrons or to a final state with  $\pi^0$  is not explicitly calculated. The spectrum of the hadronic energy from such events is similar to that from NC events. Thus we allow for such a background contribution by increasing the NC contribution by 15%, based on the calculation of the relative rates from these two sources in NuMI-L-714.

The most time consuming part of these calculations is the event generation in GNuMI. To improve statistics somewhat, each GNuMI generated event is used 4 times, varying each time the  $y$  distribution (for both NC and CC events) and the smearing of the total hadronic energy.

I do not believe that the results presented herein depend very much on the details of these approximations (except of course the detection efficiencies for the signal and background). However, if desired, the various parameters can easily be changed and the code rerun if subsequent work should warrant it.

### **Standard Conditions and Comparison with NuMI-L-714**

We first investigate the issue of optimum energy cuts for standard conditions. Those are taken as:

Horn current – 200 kA

Target position - -35 cm

Gap between horns – 7.0 m

Decay pipe length – 677.1 m

We investigate dependence of the sensitivity on the band of visible energy accepted,. The sensitivity is stated as a figure of merit (FOM) defined as:

$$\text{FOM} = N_{\text{signal}} / \sqrt{N_{\text{background}}}$$

with the background including all NC events, beam  $\pi$  events, CC  $\pi$  events and  $\pi$  decays (accounted for by augmenting the NC rate as mentioned above). The values of FOM for different energy bands are given in Table I for a total exposure of 10 kt yrs, with  $3.8 \times 10^{20}$  protons/year on target.

High/low limits	0.5 GeV	0.75 GeV	1.0 GeV	1.25 GeV	1.5 GeV
4.0 GeV	1.07	1.10	1.12	1.15	1.13
4.5 GeV	1.12	1.17	1.21	1.19	1.19
5.0 GeV	1.18	1.21	1.23	1.25	1.24
5.5 GeV	1.20	1.22	1.25	1.26	1.25
6.0 GeV	1.20	1.22	1.25	1.27	1.25
6.5 GeV	1.20	1.22	1.26	1.27	1.23
7.0 GeV	1.19	1.21	1.21	1.25	1.23

Table 1. Sensitivity (expressed as Figure of Merit) as a function of low and high visible energy cuts.

As the Table indicates, the optimum is rather shallow in the region illustrated, with a reasonable choice of cuts being 1.25 and 6.2 GeV. This is consistent with the limits indicated in Fig.13 in NuMI-L-714 for  $\Sigma m^2 = 3.0 \times 10^{-3} \text{ eV}^2$  if we use for conversion factor of 100 pe's / GeV.

The histograms of visible energy for the signal and the three sources of background are shown in Fig. 1. The beam  $\bar{\nu}_\mu$  distribution suffers somewhat from low statistics (100000 protons on target were generated) but is probably sufficient for our purposes. In these distributions we have used 1.25 and 6.2 GeV for the low and high end energy cutoffs respectively.

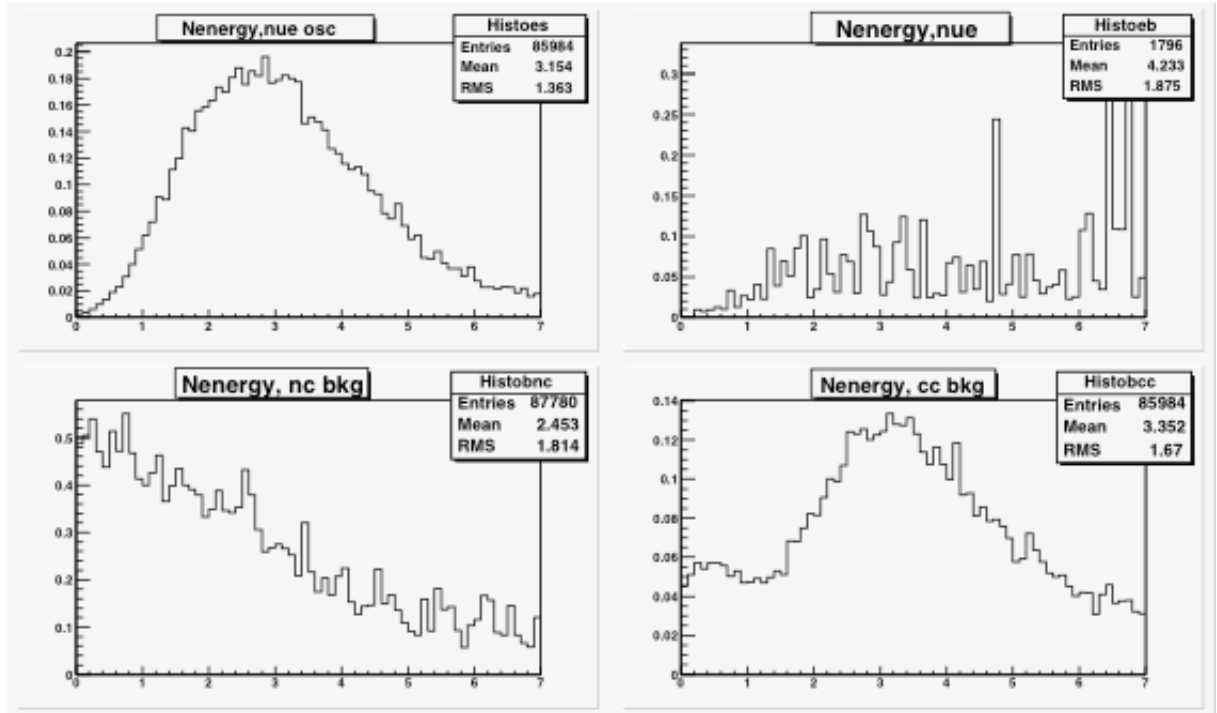


Fig.1. Histograms of signal events (upper left) and the three backgrounds : beam  $\bar{\nu}_\mu$ 's (upper right), NC events (lower left) and  $\bar{\nu}_\mu$  CC events (lower right). Standard NuMI low energy beam parameters are used. The vertical scale is in events/100 MeV in a 10 ktyr exposure, the horizontal scale visible energy in GeV.

We compare the results of these calculations with the results obtained in NuMI-L-714. The comparison is illustrated below in Table II where we list total number of events for each category and each work for integrated exposure of 10 kt yrs. The results are somewhat different in a number of ways. The overall rate is lower; this may be at least partially due to the use of different GNuMI parameters, since the input to that code has changed over the last two years. The number of NC background events is significantly lower. This is partly due to the lower normalization and partly due to the anomalously high contribution in NuMI-L-714 from the high energy events. The observed differences

appear to me to be somewhat surprising in light of the fact that our parametrizations were taken to be reasonably consistent with the corresponding values quoted in [4].

Source	Signal Oscillated $\bar{\nu}_\mu$	Backgrounds				Figure-of-Merit
		Beam $\bar{\nu}_\mu$	$\bar{\nu}_\mu$ CC	NC	$\bar{\nu}_\mu$ decay	
This work	5.8	3.0	4.3	11.7	1.8	1.27
NuMI-L-714	8.5	5.6	3.9	27.2	3.0	1.35

Table II. Comparison of the total number of events, both signal and background, for the standard NuMI low energy beam configuration for both this and previous work. The numbers correspond to a 10 kt yr exposure.

#### **Dependence on Length of the Decay Pipe**

We have studied the dependence of our sensitivity on the length of the decay pipe in the NuMI beam. The results from two runs with shorter decay lengths are compared to the current length of 677m in Table III. We have used 1.25 and 6.2 GeV as the lower and higher energy cutoffs for the accepted events.

Decay Pipe Length	Signal Oscillated $\bar{\nu}_\mu$	Backgrounds				Figure-of-Merit
		Beam $\bar{\nu}_\mu$	$\bar{\nu}_\mu$ CC	NC	$\bar{\nu}_\mu$ decay	
677 m	5.8	3.0	4.3	11.7	1.8	1.27
377m	5.4	2.9	3.8	10.8	1.6	1.25
477m	5.5	3.5	4.0	10.8	1.6	1.23

Table III. Predicted rates as function of the decay length.

As can be seen from the Table, within the range studied there is no statistically significant difference between various configuration. It is clear that one cannot improve the sensitivity significantly by shortening the decay pipe.

#### **Dependence on Horn Current**

A relatively small decrease in the horn current gives some enhancement of the flux at very low energies at the expense of flux at higher energies. We have investigated to see whether one could obtain an improvement in sensitivity by decreasing the horn current

(in both horns simultaneously). The results from runs with three different horn currents are shown in Table IV.

Horn Current	Signal Oscillated $\mu$	Backgrounds				Figure-of-Merit
		Beam $\mu$	$\mu$ CC	NC	$\mu$ decay	
200 kA	5.8	3.0	4.3	11.7	1.8	1.27
190 kA	5.3	3.3	3.8	10.4	1.5	1.22
180 kA	5.0	2.7	3.3	9.9	1.5	1.20
160 kA	4.1	3.2	2.5	9.2	1.4	1.01

Table IV. Dependence of sensitivity on horn current

It is clear that decrease of the horn current results in a slight loss of sensitivity due to the overall decrease in the neutrino interaction rate. The statistical errors on the individual rates are in the 0.5 – 2% range except on the beam  $\mu$  rate where the error is about 10%. Thus the observed decrease in FOM, even for 18 and 190 kA appears to be statistically significant.

#### **Dependence on Target Position**

We have subsequently investigated the dependence of our sensitivity on the position of the target. The other parameters have the standard values. The results for three different positions are shown in Table V.

Target Position	Signal Oscillated $\mu$	Backgrounds				Figure-of-Merit
		Beam $\mu$	$\mu$ CC	NC	$\mu$ decay	
-35 cm (standard)	5.8	3.0	4.3	11.7	1.8	1.27
-20 cm	4.8	3.8	3.1	9.7	1.5	1.13
-55 cm	6.6	4.1	5.5	13.8	2.1	1.30
-70 cm	6.9	5.8	6.4	15.6	2.3	1.25

Table V. Dependence of sensitivity on target position

As can be seen from the Table, one possibly might be able to get slight improvement by moving the target upstream somewhat.

### **Dependence on the Position of 2<sup>nd</sup> Horn**

The dependence of the sensitivity on the position of the 2<sup>nd</sup> horn is exhibited in Table VI. As can be seen, the sensitivity decreases slightly as we go away from the nominal value of 10m.

Position of 2 <sup>nd</sup> Horn	Signal Oscillated $\square_e$	Backgrounds				Figure-of-Merit
		Beam $\square_e$	$\square_e$ CC	NC	$\square_e$ decay	
10 m (standard)	5.8	3.0	4.3	11.7	1.8	1.27
8 m	5.1	3.9	3.4	9.9	1.5	1.19
12 m	5.9	4.7	4.7	12.8	1.8	1.21

Table VI. Dependence of sensitivity on the position of the second horn

### **Dependence on Target Length**

We investigated the dependence on target length by increasing the length of the target and simultaneously moving the target upstream by an amount equal to that increase. (except for the last entry). The results are shown in Table VII. For the last entry, the target position was such as to have its downstream end 15cm downstream of the nominal position.

Length of the Target	Signal Oscillated $\square_e$	Backgrounds				Figure-of-Merit
		Beam $\square_e$	$\square_e$ CC	NC	$\square_e$ decay	
0.95 m (standard)	5.8	3.0	4.3	11.7	1.8	1.27
1.15 m	6.7	3.8	5.5	12.8	1.9	1.37
1.35 m	7.3	6.1	6.8	15.3	2.3	1.33
1.3 m	6.9	3.3	5.9	13.6	2.1	1.39

Table VII. Dependence on target length (position of downstream end was kept fixed except for the last entry)

As the Table shows there is a significant increase in FOM as the target length is increased. In light of the results on variation in target position only, this is probably due both to a more optimum position and more optimum length.

### Dependence on Transverse Target Dimensions

We subsequently looked at the sensitivity of the experiment to the transverse dimensions of the target. The nominal target dimensions are 6.4 mm in width and 20.0 mm in height to be compared with the half width of the horizontal and vertical beam distributions of 0.7 and 1.4 mm respectively. The maximum beam size is given as 3.5 and 7.0 mm for these two dimensions. Thus, in principle at least, there is considerable room to decrease the transverse dimensions of the target and still contain a great majority of the beam assuming that the position of the proton beam can be maintained on the beam line. The results for several different transverse dimensions are enumerated in Table VIII. Unintentionally, these data, except for the last row, were run with target z position at  $-70$  cm.

Dimension of the Target	Signal Oscillated $\square$	Backgrounds				Figure-of-Merit
		Beam $\square$	$\square$ CC	NC	$\square$ decay	
H=10.0 mm W=6.4 mm	7.1	5.0	6.7	16.3	2.4	1.28
H=8.0mm W=6.4 mm	7.3	3.8	6.9	16.5	2.4	1.34
H=6.0 mm W=6.4 mm	7.2	5.6	6.9	16.0	2.4	1.29
H=20.0 mm W=5.0 mm	7.2	4.8	6.9	17.1	2.6	1.29
H=20.0 mm W=4.2 mm	7.0	5.1	6.6	15.6	2.3	1.29
H=20.0 mm W=3.5 mm	7.0	4.3	6.7	16.1	2.4	1.28
H=8.0 mm W=4.5 mm L=1.15 m	7.0	3.0	5.9	14.4	2.2	1.38

Table VIII. Sensitivity to transverse target dimensions

The data shown in Table IX shows that the sensitivity might be improved slightly by reducing the target transverse dimensions. Eventually one has to have decrease of sensitivity due to the tails of the beam missing the target. For completeness, we show in the last entry of the Table the sensitivity obtained when one uses the apparent optimum values for all three target dimensions. The position of the target is moved upstream by 20 cm to leave its downstream end in the nominal position. There does not appear to be significant improvement over the nominal transverse dimensions.



### **Sensitivity to Energy Resolution**

The measured (and calculated) energy resolutions for electrons and hadrons in the MINOS detector are about 22% and 55% respectively. We have used 45% in our calculations above as a compromise between these two values and also to allow for possible additional contribution due to the fact that we are looking at a neutrino interaction. It is possible that our resolution will be somewhat better since we are preferentially selecting events with a large fraction of the final state energy going into the electron. Accordingly, we have redone our Table I with the energy resolution taken as 32%. The results are shown in Table IX.

High/low limits	0.5 GeV	0.75 GeV	1.0 GeV	1.25 GeV	1.5 GeV
4.0 GeV	1.09	1.10	1.16	1.18	1.17
4.5 GeV	1.15	1.20	1.24	1.23	1.26
5.0 GeV	1.20	1.23	1.26	1.30	1.28
5.5 GeV	1.22	1.23	1.28	1.30	1.29
6.0 GeV	1.21	1.24	1.28	1.30	1.30
6.5 GeV	1.21	1.24	1.28	1.28	1.24
7.0 GeV	1.20	1.22	1.22	1.26	1.25

Table IX. Sensitivity as function of lower and higher energy cuts for an improved energy resolution (32%)

As can be seen from the above Table our sensitivity is improved only slightly, by about 2%.

### **Statistical Significance**

The statistical uncertainty in the above calculation originates in two sources. Firstly, there will be fluctuations in the generations of the GNUMI data sets. Secondly there will be fluctuations due to the imposition of experimental resolution on top of the true GNUMI values. To indicate the magnitude of these effects we have generated three different GNUMI data sets using the parameters of the last entry in Table VIII and for each data set we performed two runs with different variation away from the true values. The results are shown in Table X.

As can be seen from the Table, the statistical precision on our results is of the order of 1-2% on the Figure of Merit. The major contribution to this uncertainty comes from the beam  $\bar{\nu}_\mu$  charged current background that is calculated with a precision of 5-10% and to a lesser extent from the neutral current background. Thus the statistical precision would have profited from larger GNUMI data sets.

### **Origin of signal and background events**

In Fig.2 we display the true neutrino energy for our accepted signal and background events, the latter displayed separately for the different sources.

Data Set	Signal Oscillated $\bar{\nu}_\mu$	Backgrounds				Figure-of-Merit
		Beam $\bar{\nu}_\mu$	$\bar{\nu}_\mu$ CC	NC	$\bar{\nu}_\mu$ decay	
1st	6.95	2.99	5.94	14.34	2.15	1.376
	6.94	3.05	5.94	14.77	2.22	1.374
2nd	7.03	3.59	6.06	14.73	2.21	1.362
	7.00	3.61	6.06	13.94	2.09	1.358
3rd	6.95	4.07	5.93	13.90	2.08	1.362
	6.97	4.04	5.95	13.65	2.05	1.368

Table X. Comparison of several different runs with the same GNuMI geometry

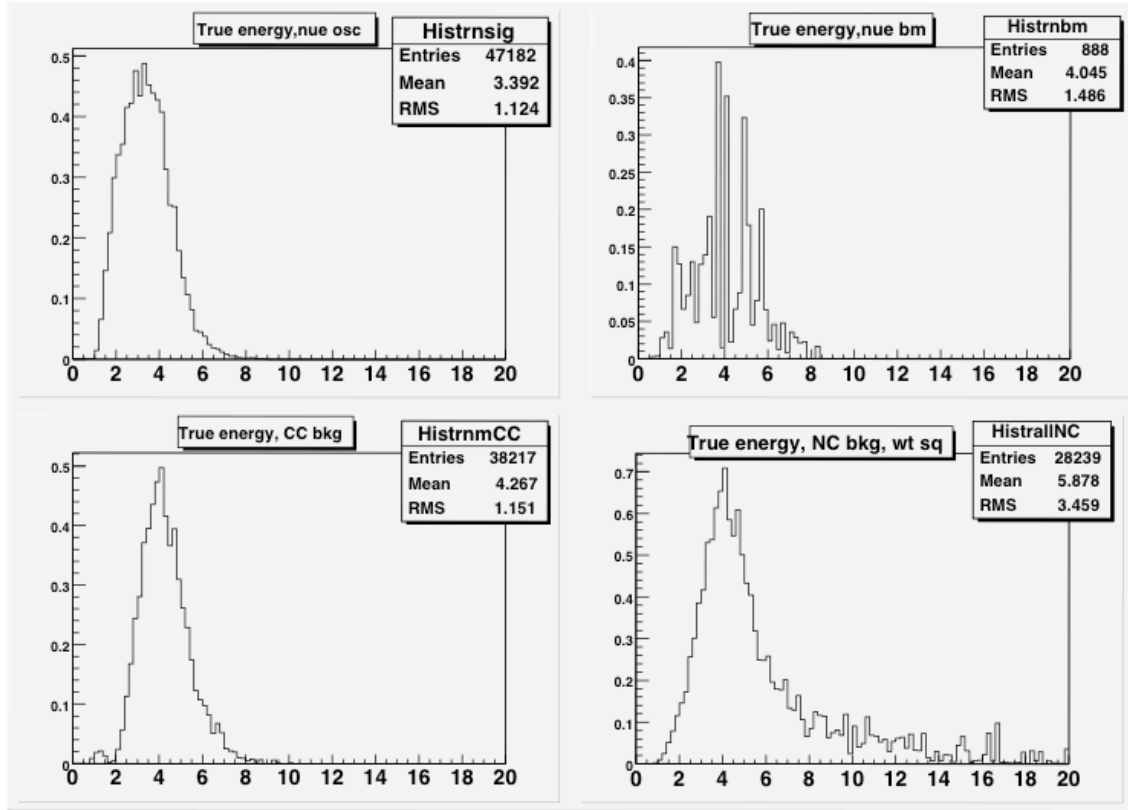


Fig.2. True neutrino energy of the signal events (upper left),  $\bar{\nu}_\mu$  beam CC events (upper right),  $\bar{\nu}_\mu$  CC events (lower left), and NC events (lower right)

The most significant observation to make is that the contribution from high energy NC events is rather low. This is in marked contrast with the result of NuMI-714 but is not surprising considering the procedure we have adopted to calculate the backgrounds.

### **Conclusion**

We have presented a study of the dependence of MINOS  $\bar{\nu}_\tau \rightarrow \nu_\tau$  sensitivity on a number of geometrical parameters using generation of the beam spectra via GNuMI and a parametrized description of the measurement smearing. In general the beam conditions appear to be reasonably well optimized; the one area where some gain might be achieved (at the level of 10% or so in the Figure of Merit) is in the dimensions and position of the target.

Comparison is made with a previous GEANT based study described in NuMI-714. Aside from the expected differences due to a different version of GNuMI used, there is a significant difference in the amount of predicted NC background due to high energy events, our study giving a lower contribution. At the present time it is not understood which study gives a more accurate answer.

### **References**

- 1) CHOOZ Collaboration, M. Apollonio et al., Phys. Lett. B **466**, 415
- 2) For a recent compilation of data as well as theoretical discussion see P. Lipari, Nucl. Phys. B (Proc. Suppl.) **112** (2002) 274
- 3) S. Wojcicki, NUMI-NOTE-SIM-290, Identification of Electromagnetic Showers in a Hadronic Shower
- 4) M. Diwan, M. Messier, B. Viren, L. Wai, NUMI-NOTE-SIM-0714, A study of  $\bar{\nu}_\tau \rightarrow \nu_\tau$  sensitivity in MINOS